

Is the black hole in NGC 1277 really over-massive?

Eric Emsellem,^{1,2*}

¹*European Southern Observatory, Karl-Schwarzschild-Str. 2, 85748 Garching, Germany*

²*Université Lyon 1, Observatoire de Lyon, Centre de Recherche Astrophysique de Lyon
and Ecole Normale Supérieure de Lyon, 9 avenue Charles André, F-69230 Saint-Genis Laval, France*

30 October 2018

ABSTRACT

A recent claim has been made by van den Bosch et al. (2012) that the fast-rotator galaxy NGC 1277 hosts an over-massive black hole with a mass ($1.7 \cdot 10^{10} M_{\odot}$) larger than half its (central) stellar spheroid mass. We revisit this claim here by examining the predictions from simple dynamical realisations based on new Multi-Gaussian Expansion models of NGC 1277, using the same inclination $i = 75^{\circ}$, and constant mass-to-light ratios. We present realisations which fit well the observed photometry taking into account an approximation for the extinction due to the central dust ring. The mass-to-light ratio M/L is fixed following scaling relations which predict a Salpeter-like IMF for such a luminous early-type fast rotator, 60% higher than the one of the previously derived best fit model. A model without a black hole provides a surprisingly good fit of the observed kinematics outside the unresolved central region, but not, as expected, of the central dispersion and Gauss-Hermite h_4 values. A model with a black hole mass of $5 \cdot 10^9 M_{\odot}$ allows to fit the central dispersion profile, consistently with models of the same mass and M/L in van den Bosch et al. (2012). It departs from the central h_4 values by only about twice the given uncertainty. A slightly varying M/L or the addition of high velocity stars in the central spatially unresolved region would further lower the need for a very massive black hole in the central region of NGC 1277. These results do not, by themselves, rule out the presence of a presumed over-massive black hole at the centre of NGC 1277. However, they lead us to advocate the use of three- σ (as opposed to one- σ) confidence intervals for derived M_{BH} as better, more conservative, guidelines for such studies. We also caution for the use of ill-defined spheroidal components as an input for scaling relations, and emphasise the fact that a M_{BH} in the range $2 - 5 \cdot 10^9 M_{\odot}$ would represent less than 5% of the spheroid bulge-like mass of our models and less than 2.5% of its total stellar mass. This would make the black hole in NGC 1277 consistent or just twice as large as what a recent version of the $M_{\text{BH}}-\sigma$ predicts, well within the observed scatter. We examine the impact of the presence of an inner bar by running simulations from the same MGE model but with extreme anisotropies. An inner small (600 pc diameter) bar forms, and an end-on view does get closer to fitting the central dispersion profile (and fits the h_3 amplitude) without the need for a central dark mass, while adding a black hole of $2.5 \cdot 10^9 M_{\odot}$, in line with the prediction from scaling relations, allows to fit the dispersion peak and h_3 profiles. Both models, however, still fail to fit the central h_4 value (overpredicting the mean velocity). The claimed large mass of the presumed black hole therefore mostly relies on the measured positive high central h_4 (at high dispersion), which can be associated with broad wings in the Line-Of-Sight-Velocity Distribution (high velocity stars). This emphasises the need to go beyond medium resolution long-slit kinematics, with e.g., high resolution integral-field spectroscopic data. In the specific case of NGC 1277, molecular or ionised gas kinematics (if present) within the central arcsecond (or at large scale) may provide a strong discriminant between these various models. We finally briefly discuss the fact that NGC 1277 resembles a scaled-up version of e.g., NGC 4342, another nearly edge-on fast rotator with a potentially large (but not over-massive) black hole.

Key words: galaxies: elliptical and lenticular, cD – galaxies: kinematics and dynamics – galaxies: structure – galaxies: nuclei

* E-mail: eric.emsellem@eso.org

1 INTRODUCTION

A recent claim has been recently made by van den Bosch et al. (2012) that the fast-rotator galaxy NGC 1277 hosts an over-massive black hole with a mass ($17 \pm 3 \times 10^9 M_{\odot}$) quoted as larger than half the stellar bulge mass. This departs very significantly from predictions of the so-called $M_{\text{BH}}-\sigma$ relation (see e.g. Tremaine et al. 2002), or the bulge-black hole mass relation. The best fit model including a relatively small size black hole ($10^8 M_{\odot}$) with respect to its spheroidal component, and using the same mass-to-light ratio, fails to fit e.g., the stellar velocity dispersion profile within the central $10''$ (see their Figure 3). This emphasises the fact that a large $17 \pm 3 \times 10^9 M_{\odot}$ black hole would influence the potential of the galaxy far out, a few hundreds of parsec from its central location. If confirmed, the existence of this over-massive black hole (relatively to the host galaxy) could either be a rare and exotic case, or would actually shed new light on the relation between the formation and evolution processes of early-type fast rotators and their central dark mass.

In this short paper, we revisit this claim by building simple dynamical models based on the Multi-Gaussian Expansion technique (Emsellem et al. 1994), also used in the modelling approach adopted by van den Bosch et al. (2012). The goal of the present paper is not to perform new fits to the observed dataset. Here, we explore further what are the main constraints motivating the need for a very large black hole mass, and wish to examine whether other slight variations in the input assumptions may help reconcile the specific case of NGC 1277 with the above-mentioned scaling relations. We also examine the potential impact of an inner bar for the observed stellar kinematics of such a fast rotator (see, e.g. Gerhard 1988), and more specifically its potential effect on the central stellar velocity dispersion. This could result in important diagnostics and in a near future help refute or confirm the claim of van den Bosch et al. (2012) (hereafter, vdB+12). In Sect. 2 we provide some basic information about the observational data and methods we have used in this paper. We then proceed in Sect. 3 to present the results coming out of this focused study, and wrap things up in Sect. 4.

2 OBSERVATIONAL DATA AND METHODS

2.1 Photometry and stellar kinematics

For the present paper, we have used of the same input photometry and stellar kinematics as in van den Bosch et al. (2012), namely:

- Images obtained with the HST/ACS in the course of the GO:10546 programme (PI Fabian) with the F550M and F625W filters. We gathered the ACS images from the ST-ECF Hubble Science Data Archive and used the PSF as derived from the TinyTim software.
- Long-slit stellar kinematics as presented in vdB+12 which consists of a major-axis profile from the LRS spectrograph mounted at the Hobby-Eberly Telescope (HET), covering up to about a radius of about $20''$ for the stellar velocity V , velocity dispersion σ , as well as for the next two Gauss-Hermite parameters h_3 and h_4 (within the central $7''$ only). The spatial resolution is about $1''.6$ Full-Width at Half Maximum (FWHM) and is parameterised with a double Gaussian model (van den Bosch et al. 2012).

The reader is encouraged to consult at the Supplementary information provided by van den Bosch et al. (2012) for further details.

2.2 MGE photometric model

The dynamical modelling relies on the Multi-Gaussian Expansion (MGE) technique developed by Emsellem et al. (1994), itself partly based on developments by Bendinelli (1991) and Monnet et al. (1992). The MGE method is a flexible way of building photometric and dynamical models of axisymmetric galaxies (see Monnet et al. 1992; Emsellem et al. 1994, for a specific treatment in the triaxial case, and deconvolution) with complex multi-component structures. A set of two-dimensional Gaussians with various widths and axis ratios is used to represent the (observed) surface brightness distribution. This MGE representation is uniquely deprojected, given viewing angles and assuming that each gaussian component is itself deprojected into a three-dimensional component constant on homothetic ellipsoids. The mass distribution can be specified by attributing a mass-to-light ratio value to each Gaussian, and including additional components (black hole, or other Gaussians which may serve as a representation for a dark halo or a gas disk).

vdB+12 have built an MGE model for NGC 1277 using the ACS F550M image and Galfit (Peng et al. 2002), the parameters of which are available in their paper (see their supplemental Table 1). We built a new MGE model this time using the HST/ACS F625W image: we do not expect that model to differ much from the one built by vdB+12 even considering the different implementation for the MGE fitting part itself. This new model should help to at least provide some partial assessment on the expected variation in the modelling. We made various fitting attempts using the pyMGE python package (Emsellem et al., in preparation; see also Cappellari (2002) for a robust idl implementation), which led to very similar outputs. During the fitting process, we masked a few bright stars and a nearby companion, and we accounted for the (apparently) roundish early-type galaxy NGC 1278 by first creating an MGE model for that galaxy which was then subtracted from the ACS image. We also attempted to mask out the region which suffered too much from the dust ring extinction visible within the central arcsecond of NGC 1277 so that our MGE model does not under-predict the amount of light at the very centre. The overall approach is similar (though not identical) to the procedure followed by vdB+12. Since we will subsequently convolve the predicted kinematics with a broad point-spread function (PSF, see below), we took into account the overall effect of the ACS PSF by approximating the corresponding TinyTim prediction with a set of two centred Gaussians.

As mentioned, the dust ring strongly affects the very central region of the surface brightness distribution (see Figure 1, or Figure 1 in vdB+12). The outer luminosity profile is also not well constrained considering the limited depth of the ACS images. In order to make sure we do not extend our MGE model significantly beyond the one built by vdB+12, and to minimise its total flux, we further constrain the two outer Gaussians to be relatively flat with an axis ratio smaller or equal to 0.7, and to have the same major-axis widths as the ones in vdB+12. The final model, normalised in flux to the F550M (for comparison) is shown in Fig. 3 (see Table 1) and compared to the one of vdB+12. Both models are surprisingly similar although, as expected, our MGE model is slightly flatter in the inner and outer parts. The fact that we imposed a flattening constraint for the largest Gaussians also prevents our MGE model from showing an abrupt change in its ellipticity in the outer parts where the observed photometry does not constrain the model well. Our MGE model has a total V -band luminosity of about $1.8 \times 10^{10} L_{\odot}$ as compared to about $2.0 \times 10^{10} L_{\odot}$ for the model of vdB+12.

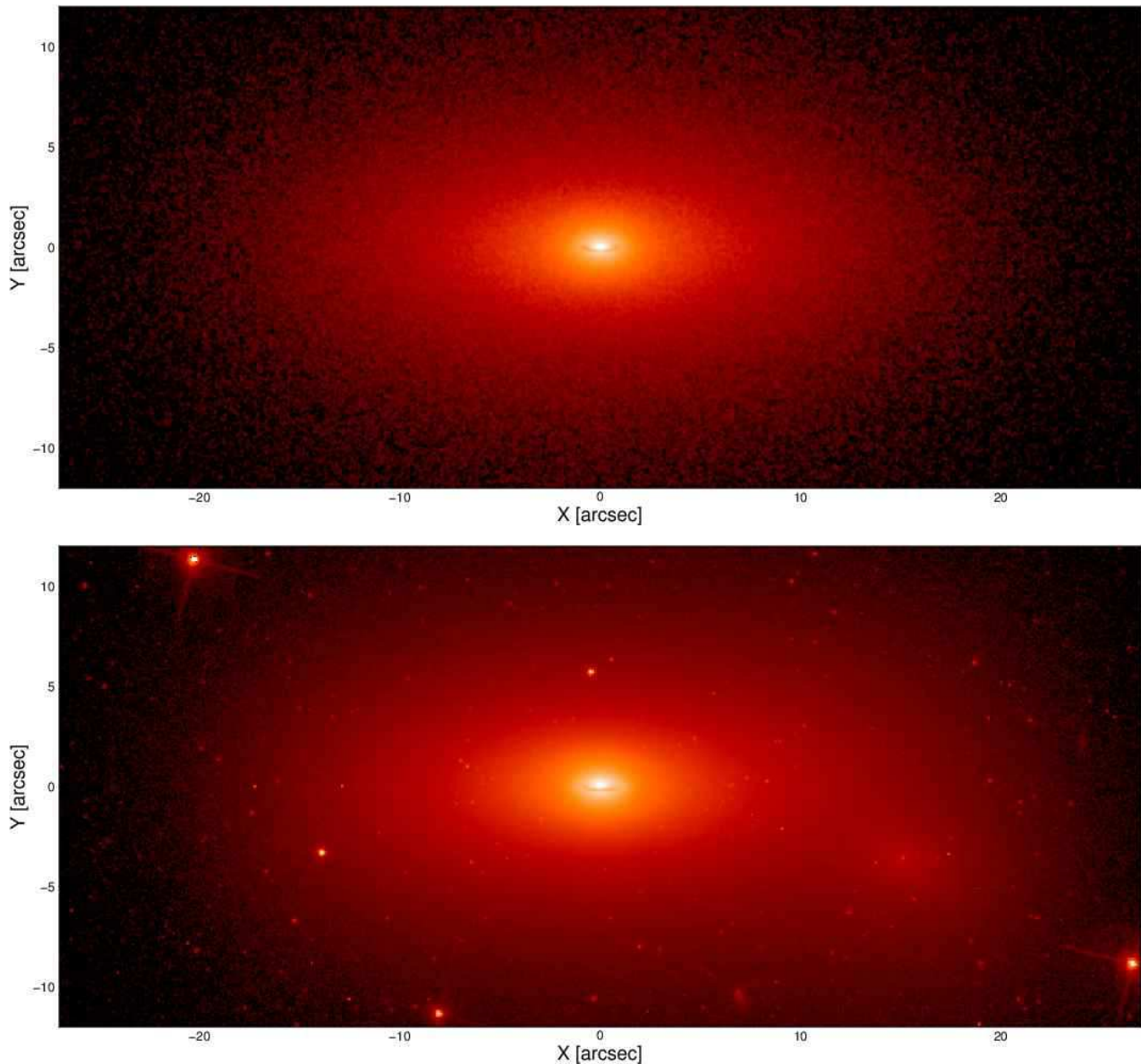


Figure 1. Reconstructed image from the MGE realisation presented in this paper (top panel) and the HST/ACS F625W data (bottom panel). The MGE model has been projected with an inclination of 75° , and assumes the presence of a small ring of dust (visible in the central arcsecond) which leads to an extinction of about 50% of the background light. A faint companion is visible in the bottom right corner of the ACS image. The graininess of the MGE model (top panel) is due to the finite number of particles included in the realisation (the corresponding analytic MGE model itself being obviously much smoother).

2.3 MGE dynamical models and comparison with observations

We built dynamical models from N-body realisations of the MGE axisymmetric models described above, using `pyMGE`. This is achieved by deprojecting the MGE models with an inclination of 75° , assuming a constant stellar mass-to-light ratio M/L for all Gaussians, and solving Jeans Equations as in Emsellem et al. (1994) and Cappellari (2008), constraining the velocity ellipsoid associated with each Gaussian to have constant axis ratios, namely σ_R/σ_z and σ_θ/σ_R (where (R, θ, z) are the cylindrical coordinates). We further added a central point-like dark mass to the gravitational potential, playing thus the role of a black hole, but no outer dark component. We kept the freedom to reverse the orbital sense of rotation of stars, as this is a way to influence the projected odd velocity moments significantly (e.g., the projected mean velocity V and h_3) without impacting the photometry (and mass) distribution. The realisations are compared with

observations by first applying a simple projection, and then taking into account the seeing Point Spread Function (PSF), pixel size and nature of the observables (photometry, kinematics via its Gauss-Hermite moments). For the kinematic quantities, we reconstructed the Line-of-Sight-Velocity Distributions with velocity bins of 25km s^{-1} steps, which are subsequently fitted using Gauss-Hermite functions up to the fourth degree leading to a measure of V , σ , h_3 and h_4 . We performed realisations using from 10^5 up to 4×10^6 particles, and we checked that the total number of particles does not significantly affect the output projected quantities.

For comparison with the HST/ACS images, we approximated the observed extinction due to the presence of a dust (and presumably gas) ring in the central arcsecond by adding a simple "screen" model: the ring itself is modelled as a circular ring of dust in the equatorial plane (between $0''.5$ and $0''.95$) and a maximum extinction factor of about 1.7 magnitude. This dust model is not meant as a realistic account of the dust extinction,

Table 1. Parameters for the reference MGE model, including the maximum amplitude for each two-dimensional (projected) Gaussian, its width in arcseconds, and its axis ratio.

#	Σ_0 $L_\odot \cdot \text{pc}^{-2}$	σ_G "	q
1	116230.070	0.0100	0.700
2	167697.701	0.0300	0.300
3	28108.207	0.0700	0.700
4	11919.362	0.1488	0.700
5	6308.461	0.2889	0.305
6	9483.126	0.3208	0.700
7	6954.700	0.6208	0.700
8	1866.762	0.9320	0.305
9	3551.888	1.2155	0.695
10	1086.092	2.6801	0.553
11	237.533	4.4573	0.286
12	344.707	6.5533	0.437
13	55.810	8.9404	0.650
14	11.970	10.5439	0.655
15	8.385	16.9824	0.655

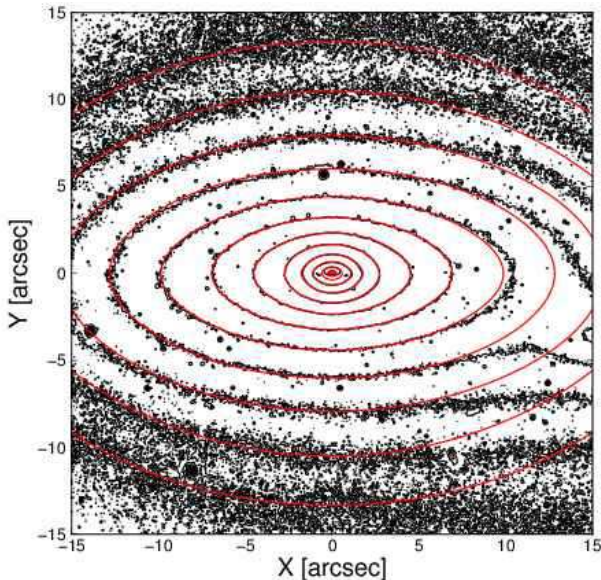


Figure 2. Isophotes of our MGE model (red contours) compared to the input HST/ACS F625W image (black contours). The influence of the galaxy neighbour in the South-West quadrant is visible already at $10''$ along the major-axis of NGC 1277.

but only as a way to get a first estimate of the effect of such a ring. This has obviously a significant effect on the reproduced HST photometry (see Figure 1), but we find that it does not have a significant impact on the observed kinematics at the spatial resolution of the HET data.

As mentioned above, we used a constant mass-to-light ratio M/L as in van den Bosch et al. (2012). We define a reference value, by simply following the known trend of more massive early-type galaxies having higher M/L (see Cappellari et al. 2006, 2012, and references therein, and e.g., Cappellari et al. 2006, Thomas et al. 2011). vdB+12 quote an aperture (within one effective radius but excluding the central arcsecond) stellar velocity dispersion of $\sigma_e \sim 333 \text{ km s}^{-1}$, and the total V -band luminosity of NGC 1277 is around $2 \cdot 10^{10} L_\odot$: this means that we expect a M/L consistent with a close to Salpeter-like initial mass function (IMF). The same is true if we refer to the mass of the galaxy which is between 1 and $2 \cdot 10^{11} M_\odot$. We therefore adopted a reference value of $M/L_V = 10$, about 60% larger than the value of 6.3 for the best fit model in vdB+12. The circular ve-

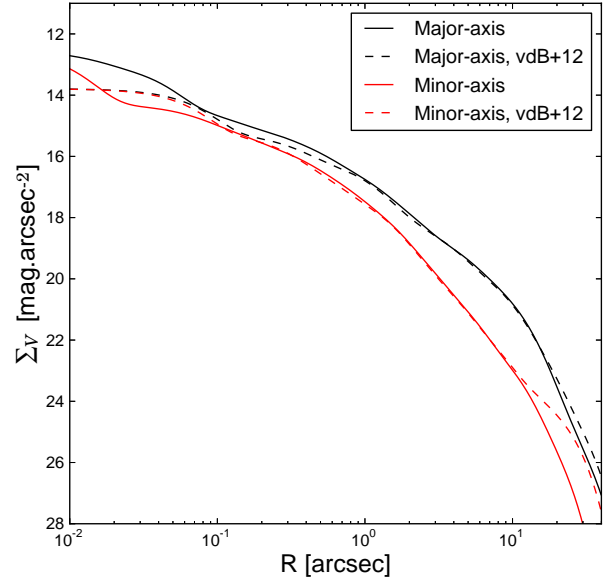


Figure 3. Major- and minor-axis photometric surface brightness cuts of the MGE models built in the present paper (solid lines), compared to the input MGE model (dashed lines) from van den Bosch et al. (2012). Profiles have been normalised to V -band surface brightness profiles for comparison.

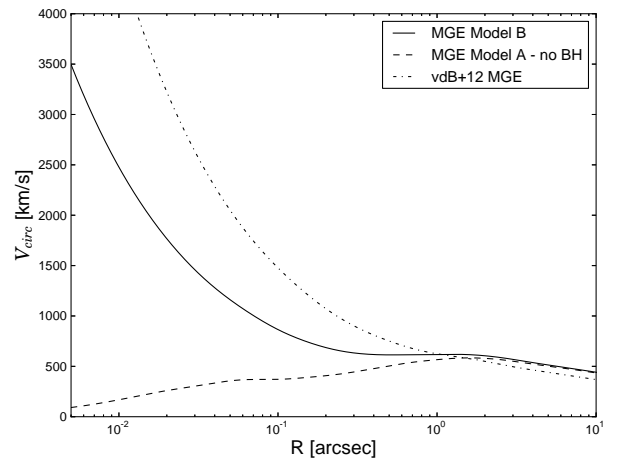


Figure 4. Circular velocity profiles for our MGE models with $M/L = 10$ and no black hole (Model A, dashed line), or a black hole mass of $5 \cdot 10^9 M_\odot$ (Model B, solid line), and the corresponding profile (dashed-dotted line) for the best fit model of van den Bosch et al. (2012) with $M/L = 6.3$ and a black hole of $17 \cdot 10^9 M_\odot$.

locity profiles in the equatorial plane for both this model (with and without a black hole) and the best fit model presented in vdB+12 (including an "over-massive" black hole of $17 \cdot 10^9 M_\odot$) are shown in Fig. 4. We should note that what drives the combined amplitudes of the stellar kinematics in the outer part (e.g., the second order velocity moment $V^2 + \sigma^2$) is the total mass, inclusive of the stars and dark matter if present. Having M/L set to a Salpeter-like IMF without a dark halo, could be thus roughly equivalent to having a lower value of the stellar M/L but adding dark matter (which would require to additionally define its relative scale, mass normalisation, and shape): this is illustrated in the shift towards higher M/L of the chi-square contours obtained by vdB+12 (Figures 1 and 3 of their Supplementary material) when removing the dark halo in the models. For a galaxy of the mass of NGC 1277, we would expect a dark matter fraction of about 15% (Cappellari et al. 2012) within one effective

radius ($5''$), and probably dominating the mass budget beyond $\sim 15''$. Since we focus here on simple models, and do not try to actually obtain best fits to the observed kinematics, we voluntarily exclude the use of an additional dark matter component in the outer part (a dark halo) or a varying M/L profile.

We used the *Gadget 2* N-body code developed by Springel (2005) to both test the stability of our MGE N-body realisations, as well as the impact of the formation of a bar. For the latter, we imposed a more extreme anisotropy with a smaller tangential dispersion σ_θ : this basically forces the model to start with dynamically cold initial conditions and is an efficient way to enforce the (artificial) triggering for the formation of a non-axisymmetric system (such as a bar).

3 RESULTS

For our reference (axisymmetric) models, we impose a simple anisotropy profile with $\sigma_R/\sigma_z \sim 1.15$ and $\sigma_R/\sigma_\theta \sim 1.4$. The first ratio corresponds to $\beta_{Rz} = 1 - \sigma_z^2/\sigma_R^2 \sim 0.25$, which is incidently consistent with the general trend found by Cappellari et al. (2007) where $\beta_{Rz} \sim 0.7 \times \epsilon_{intr}$ with ϵ_{intr} being the intrinsic ellipticity, assuming an ellipticity of about 0.3 for NGC 1277. The relatively high tangential anisotropy of the model leads to a high amplitude for the azimuthal rotation, making it a clear fast rotator (Fig. 5). We built realisations with various black hole masses using this reference model: in Fig. 6 we illustrate two models, one without a black hole ($M_{BH} = 0$, Model A), and one with a black hole ($M_{BH} = 5 \cdot 10^9 M_\odot$, Model B) twice as big as the one predicted by the $M_{BH}-\sigma$ relation recently provided by McConnell et al. (2011). Both models are stable when run with *Gadget 2* (pure N-body run with $4 \cdot 10^6$ particles with various tested softenings between 10 and 50 pc). Model B corresponds to a model which departs from the best fit model of vdB+12 at more than the $3-\sigma$ level (without a dark halo, see their Supplemental Figure 3), while we obviously expect Model A (without a black hole) to be a very poor fit of the observed stellar kinematics. In both cases we reversed the sense of rotation for about 12% of the stars for the rounder inner gaussian components, as to follow the observed skewed LOSVD (h_3 being significantly non-zero): this basically increases the azimuthal dispersion within the central $10''$ or so (see Fig. 5).

These models were not designed as actual fits for the observed stellar kinematics, but can reproduce the observed kinematics profiles rather well over most of the available radial ranges, and down to about $1''$. This may look surprising considering the very poor fit of the model with a low mass ($10^8 M_\odot$) black hole presented by vdB+12 in their Figure 3. However, that fit was constrained to have the same mass-to-light ratio than the best fit model, with a low value of 6.3, thus being very far from the best fit model without (or with a low-mass) black hole. We also compared the best fit model with $M_{BH} = 10^8 M_\odot$ (Remco van den Bosch, priv. comm.) with our Model A at the same input M/L : our model is a significantly better fit to the kinematics, but this is mostly in the outer parts while in the inner region, the two models are similar (the Schwarzschild technique provides a slightly but not significantly better fit as expected). The reason for this is certainly associated with the rounder outer Gaussians included in vdB+12 MGE model, which may render more difficult the fit of the (high V/σ) kinematics at large radii. It, however, does not invalidate the analysis in the central part. As expected, Model A (model without a black hole) does not fit the central dispersion value and has a slightly too shallow central velocity gradient. Model A, however, represents already quite a remarkable fit of the outer region down to the central $2''$. The addition of a $5 \cdot 10^9 M_\odot$ black hole (Model B) solves

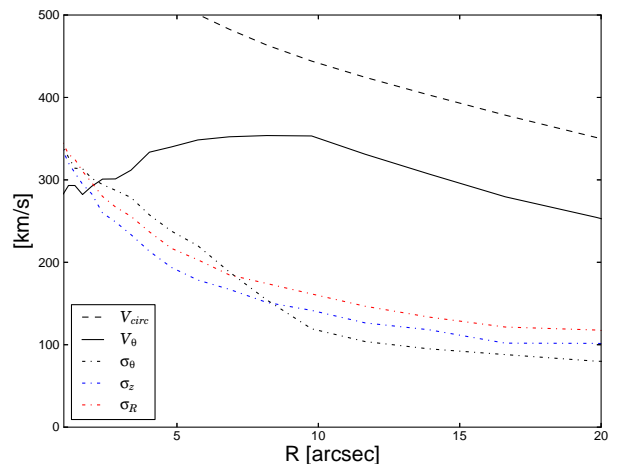


Figure 5. Velocity moments in the equatorial plane of the MGE Model B presented in this paper: the circular velocity (dashed line), mean tangential velocity (solid line) and velocity dispersion profiles (dotted-dashed lines; radial, azimuthal and vertical dispersion, respectively as red, black, and blue lines).

these two above-mentioned discrepancies. The h_3 profile is fitted rather well independently from the mass of the black hole which is used: this is mostly the consequence of the presence of about 10% of counter-rotating stars which skew the observed LOSVD. The only significant discrepancy between Model B and the observed stellar kinematics lies in the h_4 profile at the very centre, where the predicted values are slightly too low (0.0-0.02 instead of 0.04). That difference is, however, rather small, and only twice the given uncertainty on these parameters. The model of vdB+12 which corresponds to the M/L and M_{BH} values of our Model B provides a slightly better fit of the central region, while it provides a too low predicted V/σ in the outer part, again very probably due to its rounder Gaussians (a situation similar to the one described for Model A).

A high h_4 value is associated with high velocity wings of the LOSVD in the central arcsecond. A spurious h_4 value could for example originate in a so-called template mismatch (a mismatch between the galaxy spectra at these positions and the stellar template used to extract the kinematic parameters). However, if confirmed, such a high h_4 value (associated with a high central dispersion) would, for the central LOSVDs of NGC 1277, actually correspond to a few $10^8 M_\odot$ stars at velocities between 900 and 1100 km s^{-1} : these are missing in Model B. To remove that discrepancy, we could artificially add stars with high angular momentum (circular orbits) within $0''.1$ (~ 35 pc), where the circular velocity is in the right range (see Fig. 4). This would, however, lead to a significant discrepancy in the photometry (assuming a constant M/L). A more massive black hole (e.g., $17 \cdot 10^9 M_\odot$, as in vdB+12) naturally predicts the required high velocity wings by increasing the volume within which such velocities are reached. This central h_4 value is therefore a strong signature of large mass excess in the region unresolved by the HET spectroscopy, and is (as expected) a strong discriminant between models with various black hole masses.

We also examined the impact of the presence from a potentially small bar in these models by running *Gadget 2* N-body simulations with more extreme anisotropies, this time setting up the black hole mass to zero (Model C) or to a value of $2.5 \cdot 10^9 M_\odot$, consistent with scaling relations (Model D). As mentioned in Sect. 2.3, we force a small tangential anisotropy dispersion by setting a high value of σ_R/σ_θ , namely 2.0 here. With such initial conditions a small bar quickly forms after a few dynamical times in the simulation, and stays as long the simulation was run (200 Myr). The extent of the bar is small, with a diameter of

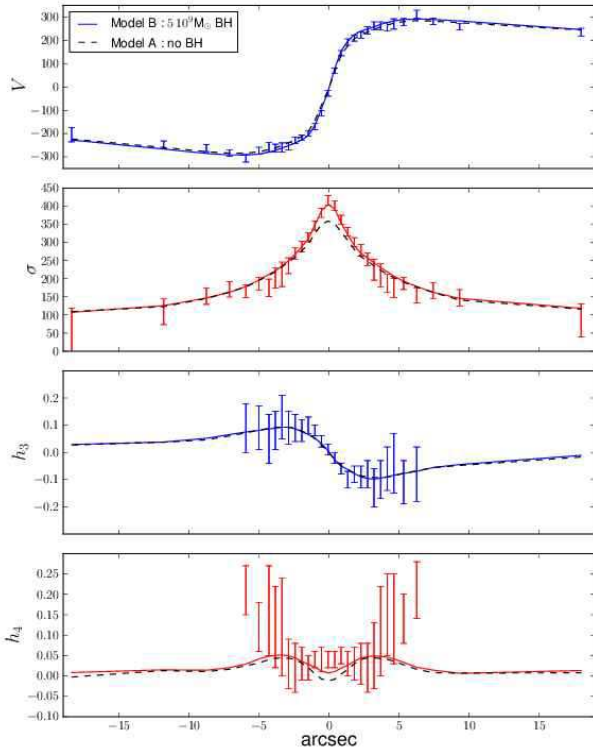


Figure 6. Kinematics from the HET long-slit data (van den Bosch et al. 2012), compared with the two models discussed in the present paper (Model B with a black hole mass of $5 \cdot 10^9 M_{\odot}$, as solid lines, and Model A without a black hole as dashed lines). This figure corresponds to Figure 3 of van den Bosch et al. (2012).

about 600 pc, as illustrated in the face-on view in Fig. 7. When the bar is edge-on (and the model inclined at 75°), the photometry is clearly not consistent with the observed photometry. With the bar seen end-on, the fit to the photometry is rather good as shown in Fig. 8, which is a bit surprising considering the significant mass redistribution triggered by the formation of the bar.

We then compare the end-on and edge-on views of these two models (Model C and D) with the observed stellar kinematics of van den Bosch et al. (2012) in Fig. 9. Using the same mass-to-light ratio $M/L_V = 10$, we get a reasonable fit of the global profiles even though this model is now, as expected, slightly under-predicting the velocity dispersion and over-predicting the mean velocity. An end-on view of the bar leads to an increase in the central dispersion peak which gets close to the observed values (385 instead of 415 km s^{-1}) for Model C and fits the dispersion peak for Model D. It is only a relative surprise considering that an end-on bar has already been discussed more than twenty years ago as a potential way to maximise the observed velocities of stars (Gerhard 1988). It is also interesting to note that, in both models, the end-on bar naturally produces a significant kink in the h_3 profile which follows rather closely the observed radial profile without the need for counter-rotating stars as in Model A and B. Ironically, the fit to the h_4 profile is reasonably good when the bar is near edge-on, but with the predicted central h_4 becoming negative for an end-on view. Again, the central h_4 seems to be the most constraining observed parameter for the presumed central dark mass. Obtaining a fit using such an evolved (barred) model is clearly beyond the scope of this paper. Results from Model C and D seem to indicate, however, that the presence of such a non-axisymmetric system may eventually lower the required central dark mass (even though the coexistence of a central dark mass and an inner 600 pc bar would have to be explained). It is worth

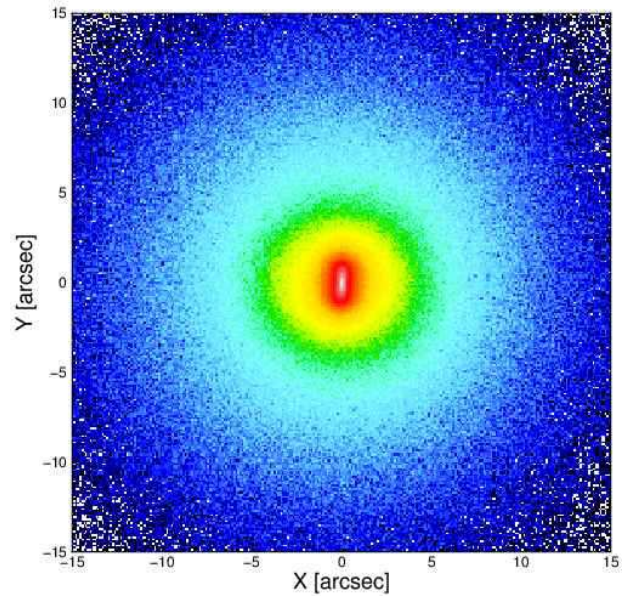


Figure 7. Face-on view of the central region of Model C after 160 Myr of evolution: the mini-bar is clearly visible here with a diameter of about 600 pc.

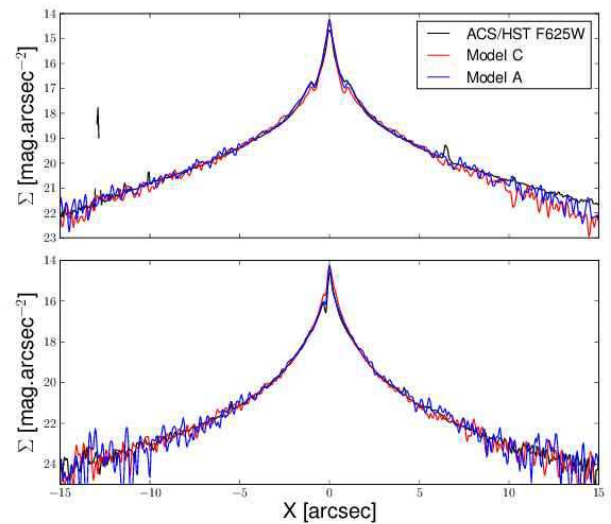


Figure 8. Cuts along the major and minor-axes of Model C after projecting the bar end-on (red profiles) and compared with the ACS/HST F625W surface brightness profiles.

noting that the bar which forms in these models would be located just inside the observed dust ring: this is very probably just linked with the fact that the circular velocity of Model A (axisymmetric model, and no black hole) peaks near a radius of $1''$.

4 DISCUSSION AND CONCLUSIONS

In this short paper, we revisit the recent claim for the presence of an over-massive black hole in NGC 1277 by van den Bosch et al. (2012). We build new MGE models which fit the photometry, using an approximation for the extinction of the observed dust ring, and assuming a fixed $M/L = 10$ consistent with a Salpeter IMF, and a nearly constant anisotropy.

We show that a model without a black hole does indeed not fit the central dispersion and h_4 values, as expected, but

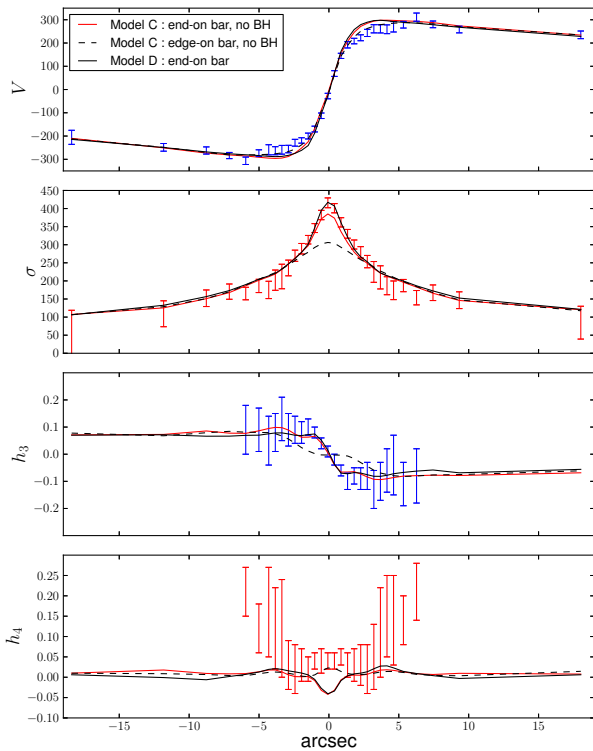


Figure 9. Comparison of the predicted stellar kinematics of Model C with the bar end-on (red lines) and edge-on (dashed black lines), and the end-on view of Model D (black solid lines) as compared with the observed kinematics from van den Bosch et al. (2012, errors bars). Note that Model C has no black hole, and Model D one with $M_{\text{BH}} = 2.5 \times 10^9 M_{\odot}$.

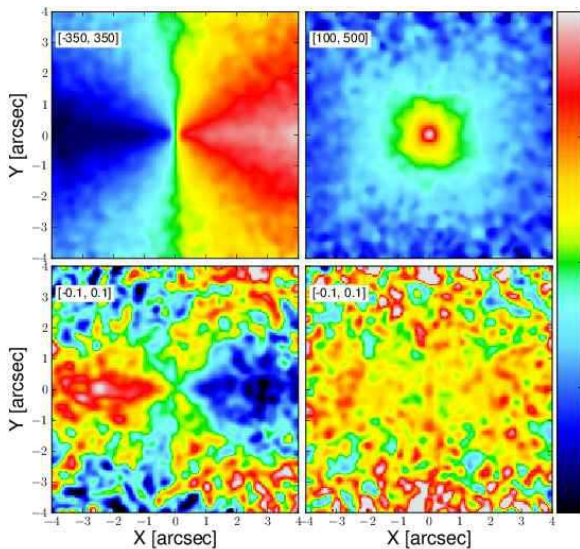


Figure 10. Predictions from Model B for the stellar mean velocity V (top left), velocity dispersion σ (top right), h_3 and h_4 fields (bottom left and right, respectively) at a resolution of $0''.3$ FWHM. V reaches about 300 km s^{-1} , the dispersion peaks at around 500 km s^{-1} , h_3 reaches between 0.075 and 0.1 and h_4 is fairly constant with values around 0.03 – 0.04 . Cuts (min/max) are: $\pm 350 \text{ km s}^{-1}$ for V , $100/500 \text{ km s}^{-1}$ for σ , and ± 0.1 for the h_3 and h_4 maps. The inclination angle is 75° .

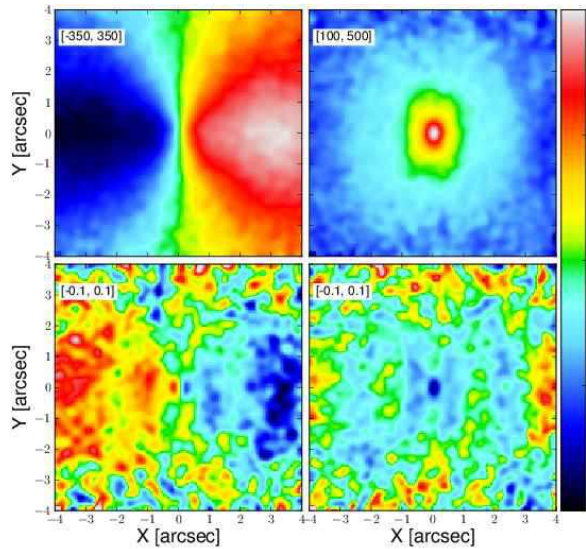


Figure 11. As in Fig. 10 but for the (end-on) barred Model D. The predicted central dispersion again reaches $\sim 500 \text{ km s}^{-1}$, not making it a strong discriminant between the models with or without such bars. However, the elongated shape of the dispersion peak could help constraining the black hole mass, as well as the two-dimensional shape and amplitude of the high order moment maps. In the present plot, h_3 goes up along the major-axis at 0.06 close to the centre (with a local minimum around $2''$ away along the major-axis), and h_4 is close to zero everywhere or slightly negative. The inclination angle is 75° .

still provides a rather good global fit of the observed long-slit kinematics. The corresponding models (with similar M/L and M_{BH} values) of vdB+12 have some difficulty to follow the high V/σ values observed in the outer parts: this may be partly linked with the intrinsic flattening of the outer Gaussians, and the flatter external components of our MGE models seem to significantly improve the situation in this context. The model with a very low M_{BH} value presented in Figure 3 of vdB+12 corresponds to the (low) mass-to-light ratio of their overall best fit model. It is clearly a very bad fit to the observed kinematics over nearly the entire radial range. However, this may be somewhat misleading as it naturally emphasises the tension between models with and without a central dark mass, not following the ridge of minimum chi-squared in the M/L - M_{BH} diagrams in vdB+12. We find it remarkable that a model with a constant M/L following observed scaling relations, simple anisotropy profiles, and no black hole provides a rather reasonable fit to the large-scale (major-axis) stellar kinematics of the galaxy except for the central arcsecond. The addition of a $5 \times 10^9 M_{\odot}$ central dark mass removes most of the discrepancy with the central stellar velocity dispersion value, and has a predicted h_4 value within two times the quoted uncertainty on that parameter.

We must emphasise again that the models presented in this paper are not actual fits to the data, but only MGE models which fit the photometry and include simple assumptions for its mass-to-light ratio and anisotropy: they can therefore not lead to a direct statement with respect to the “best-fit” value for M_{BH} , and the value claimed by van den Bosch et al. (2012). By construction, the Schwarzschild technique does find the best fit value given a set of assumptions (e.g., MGE model). Still, there are reasons to doubt the strict validity of the confidence interval for the M_{BH} value derived by Schwarzschild modelling. Some doubt may be raised when we witness the difficulty of the $M/L = 10$ models of vdB+12 to fit the outer high V/σ values very probably due to the roundish outer Gaussians of their MGE models. In that context, the role of the black hole becomes very prominent as to allow the flexibility (with a lower M/L value) to fit the entire

radial range. The addition of dark matter, if in a spherical halo, should not impact much on these issues, except by lowering the need for a high M/L to fit the overall amplitude of the kinematics (e.g., $V^2 + \sigma^2$) in the outer part. Looking at the simple parameterisation of Model A (constant M/L , no black hole) and the overall quality of the fit it provides outside the central $2''$, it is tempting to use an argument in the spirit of Occam’s razor to discard a very high M_{BH} for NGC 1277. Since chi-square contours should provide (as presented in vdB+12) an objective assessment of the quality of the fits, but do not include the systematic changes which could be triggered by a change in the MGE model itself (via e.g. different Gaussians, or a slightly varying M/L), we believe that it solely means that we should be more conservative and advocate to quote uncertainties corresponding to $3\text{-}\sigma$ confidence levels instead (which would nearly include Model B), namely the best fit value of $17\ 10^9\ M_{\odot}$ (vdB+12) but a range $[5 - 25]\ 10^9$.

We now briefly comment on the mass ratio between the black hole and spheroidal component of the galaxy. van den Bosch et al. (2012) find that a $17\ 10^9\ M_{\odot}$ black hole would represent 59% of the central bulge-like component. However, this directly relies on the definition of what should be the “bulge” fraction of the galaxy (central or global component). By focusing on a specific scale, and thus a presumed central component, there is a risk that such a fraction is artificially set on the high side. This again depends on a given scale and the (difficult) identification of what we should call a bulge. Since there is a direct connection between a given M/L and the corresponding best fit M_{BH} (see supplemental Figures 1 and 3 of vdB+12), it obviously also depends on the M/L itself (and the fraction of dark matter in the outer region), which directly influences the bulge mass. To further quantify this using our MGE model (with $M/L = 10$), and assuming we now identify the spheroidal component to be the sum of all Gaussians with axis ratios larger than 0.3, we find a mass of $\sim 1.8\ 10^{11}\ M_{\odot}$. If we focus only on the more central spheroidal components (within e.g., 2 kpc) this would amount to about $\sim 10^{11}\ M_{\odot}$. The large value advocated by van den Bosch et al. (2012) for the black hole would thus represent between 10% and 20% of these masses, already significantly lower than the mentioned value of 59%. Such an estimate would not be significantly impacted by the presence of about 15% of dark matter within one effective radius. With a lower M_{BH} of $5\ 10^9\ M_{\odot}$ as for Model B of the present paper, this would correspond to either 3% or 5%, putting it in a range similar to what was derived for e.g., NGC 4342 Cretton & van den Bosch (1999). With a measured σ of $333\ \text{km s}^{-1}$ van den Bosch et al. (2012), the latter value for M_{BH} would make the black hole in NGC 1277 only twice bigger than what a recent version of the $M_{\text{BH}}\text{-}\sigma$ relation predicts McConnell et al. (2011), well within the measured scatter. NGC 1277 would then again resemble a scaled-up version of e.g., NGC 4342, another close to edge-on fast rotator with a relatively large black hole: the fact that these are two, close to edge-on, fast rotators is an interesting fact to emphasise. In both cases, the spheroidal component contributes significantly to the overall rotational support of the galaxy, with a relatively small tangential anisotropy (at least near the equatorial plane).

We have also presented an illustration of the impact of an inner bar in such models (Model C and D) and showed that the predicted central dispersion value could get relatively close (within 8%) to the observed value when such a mini-bar is viewed close to end-on, even without a central dark mass (the model fitting the dispersion peak when $M_{\text{BH}} = 2.5\ 10^9\ M_{\odot}$). Such models naturally reproduce the relatively high h_3 amplitude, but fail to reproduce the observed positive central h_4 value. We cannot comment further at this stage about the possibility of

fitting all observed kinematics simultaneously with a bar, as this would require more finely tuned models to understand whether or not the central h_4 value is obtainable for such systems. It is, however, probable that a central mass (of a few $10^9\ M_{\odot}$) would anyway be required if the high positive h_4 value is confirmed, as it corresponds to broad wings in the central LOSVDs, thus stars moving at speeds significantly above the predicted circular velocity (see Fig. 4).

This work emphasises the fact that the high value claimed for the mass of the central dark mass, as quoted in van den Bosch et al. (2012), therefore mostly relies on the robustness of the central (significantly positive) h_4 value. This seems quite natural considering that a high h_4 can be the direct consequence of e.g., a high central mass concentration. The differences (in the high velocity wings of the LOSVDs) between our model with a $5\ 10^9\ M_{\odot}$ black hole and the measured central h_4 values cumulate to about $5\ 10^8$ of stars rotating at about $1000\ \text{km s}^{-1}$. According to the predicted circular velocity profiles shown in Fig. 4, this could correspond to a concentration of high angular momentum stars within the central 70 and 25 pc for M_{BH} of 17 and $5\ 10^9\ M_{\odot}$, respectively: in the latter case, such a structure would not be resolved but should be detectable with integral-field spectroscopy and adaptive optics or obtained in excellent seeing conditions. Predictions from Model B and D for integral-field kinematics of the central few arcseconds at high resolution (Full Width at Half Maximum, FWHM, of $0''.3$) are provided in Figs. 10 and 11: the shape of the central stellar velocity dispersion peak (at that resolution), as well as the higher order moments should be strong discriminants between these various models as well as to further constrain the black hole mass. Black holes of $2.5\ 10^9$ and $5\ 10^9\ M_{\odot}$ would imply a very peaked central dispersion reaching about 445 and $500\ \text{km s}^{-1}$ respectively, at that resolution. We should expect a significantly more massive black hole as advocated by vdB+12 to produce an even more extreme dispersion peak, reaching well beyond $500\ \text{km s}^{-1}$. A central bar may show up a distinct kink in the h_3 map within $2''$ with local minima along the major-axis (see Fig. 11).

It may be difficult to rule out a lower mass black hole using potential ionised or molecular gas associated with the dust ring, as this ring has a diameter close to $1''$ where the circular velocity profiles of the various models (see Fig. 4) overlap, so that any interpretation would depend on the detailed characteristics of the gaseous orbits (circular or not). A proper test would again require two-dimensional spectroscopy (see e.g. Krajnović et al. 2005) at high spatial resolution to probe the central few tenth of arcseconds¹. Another way to start discriminating between these models would be if ionised gas is detected at *larger* radii (beyond a few arcseconds) where the circular velocity profile is assumed to be dominated by the stellar component and where the actual mass-to-light-ratio would have strong predictive power.

Finally, we would like to emphasise the resemblance between a galaxy like NGC 1277 and NGC 4342, which had been studied by Cretton & van den Bosch (1999) who claimed for the presence of supermassive black hole which represents about 3% of the total spheroid mass, one of the largest black hole mass to bulge mass known at the time. NGC 4342 is a close to edge-on fast rotator with a prominent inner disk and stellar kinematics which show similar radial major-axis profiles (though with different amplitudes), specifically with an extended dispersion profile (van den Bosch et al. 1998). The derived best fit model has anisotropy profiles (see Figure 13 of Cretton & van den Bosch 1999) which are very similar to

¹ Gemini/NIFS data has now been obtained (PI: Richstone), and should help tremendously in this context.

the ones derived for NGC 1277 here (Fig. 5) with σ_θ being lower in the outer part than the two other components of the velocity ellipsoid, while going up in the central region above σ_R , and σ_R/σ_z being rather constant around 0.9. It is not surprising to note that, according to the model of NGC 4342 presented in Cretton & van den Bosch (1999), the rise of σ_θ in the inner part corresponds to the observed rise in the stellar velocity dispersion. Cretton & van den Bosch (1999) also noted that the mass-to-light ratio derived from their best fit model is large relatively to other early-type galaxies. NGC 1277 can thus roughly appear as a scaled-up version of NGC 4342 (factor of about 8 in mass). Interestingly, the potential presence of an end-on bar was discussed for NGC 4342 by Cretton & van den Bosch (1999), to acknowledge the similarities with another fast rotator, NGC 4570, where evidence for bar-driven secular evolution (van den Bosch & Emsellem 1998) was found. Cretton & van den Bosch (1999) considered the hypothesis of an end-on bar in NGC 4342 unlikely, reflecting on the fact that the end-on view would be rather constrained, and because the cuspy luminosity profile of NGC 4342 would probably prevent the formation of a bar in the first place (see the brief discussion in their Sect. 7.2.2). These two arguments could also apply to NGC 1277 and NGC 4570, while it is worth emphasizing that the latter is also very cuspy and there are evidences for NGC 4570 to have been shaped by the presence of a bar. One common denominator of both NGC 4342 and NGC 4570 is the presence of a thin disk at a scale of about 100 pc, and NGC 4570 harbours a relatively young (~ 2 Gyr old) and very thin stellar ring at a radius of 140 pc. In NGC 1277, there is a clear ring-like dust structure at a radius of about $0''.9$ (~ 320 pc, at a distance of 73 Mpc), blocking part of the view of the very central structure. We cannot comment further to whether or not these structures are various stages of an evolution process (see also the beautiful and puzzling case of NGC 1332, presented in Rusli et al. 2011), but while searching for massive black holes in fast rotators with similar morphologies (and inclination), it would be worth keeping these facts in mind.

ACKNOWLEDGEMENTS

I would like to warmly thank Davor Krajnović for his helpful remarks on an early version of the manuscript, as well as Michele Cappellari, and Glenn van de Ven for their input. I would like to specifically acknowledge very valuable feedback from Remco van den Bosch, including on the details of the Schwarzschild models presented in vdM+12, and thank him for the open and interesting discussions we had. I wish to thank the anonymous referee for very constructive comments.

REFERENCES

- Bendinelli, O. 1991, ApJ , 366, 599
 Cappellari, M. 2002, MNRAS , 333, 400
 Cappellari M., 2008, MNRAS, 390, 71
 Cappellari, M., Bacon, R., Bureau, M., et al. 2006, MNRAS , 366, 1126
 Cappellari, M., Emsellem, E., Bacon, R., et al. 2007, MNRAS , 379, 418
 Cappellari, M., Scott, N., Alatalo, K., et al. 2012, arXiv:1208.3522
 Cretton, N., & van den Bosch, F. C. 1999, ApJ , 514, 704
 Emsellem, E., Monnet, G., & Bacon, R. 1994, A&A , 285, 723
 Gerhard, O. E. 1988, MNRAS , 232, 13P
 Krajnović, D., Cappellari, M., Emsellem, E., McDermid, R. M., & de Zeeuw, P. T. 2005, MNRAS , 357, 1113
 McConnell, N. J., Ma, C.-P., Gebhardt, K., et al. 2011, Nature , 480, 215
 Monnet, G., Bacon, R., & Emsellem, E. 1992, A&A , 253, 366
 Springel, V. 2005, MNRAS , 364, 1105
 Peng, C. Y., Ho, L. C., Impey, C. D., & Rix, H.-W. 2002, AJ , 124, 266
 Rusli, S. P., Thomas, J., Erwin, P., et al. 2011, MNRAS , 410, 1223
 Thomas, J., Saglia, R. P., Bender, R., et al. 2011, MNRAS , 415, 545
 Tremaine, S., Gebhardt, K., Bender, R., et al. 2002, ApJ , 574, 740
 van den Bosch, F. C., Jaffe, W., & van der Marel, R. P. 1998, MNRAS , 293, 343
 van den Bosch, F. C., & Emsellem, E. 1998, MNRAS , 298, 267
 van den Bosch, R. C. E., Gebhardt, K., Gültekin, K., et al. 2012, Nature , 491, 729